Trajectory Planning for UAVs equipped with RISs to Provide Aerial LoS Service for Mobile Nodes in 5G/Optical Wireless Communication Networks

Mohsen Eskandari, Andrey V. Savkin

***Abstract*—Modern wireless communication systems are limited to line-of-sight (LoS) links due to high path loss and blockage issues in millimeter wave (5G) and beyond in optical/visible light communication networks. This letter proposes utilizing (optical) reconfigurable intelligent surface (RIS)-equipped UAV (RISeUAV) to support indirect aerial LoS (ALoS) links for mobile vehicles that deliver critical metropolitan emergency/security services. The RISeUAV performs as an aerial transponder and reflects optical and wireless communication signals in dense urban areas. The navigation problem of the RISeUAV is nontrivial where RISeUAV should be autonomously navigated through an energy-efficient obstacle-free path. Notably, the flight altitude should be relatively low to ensure the quality of ALoS service while the maximum possible ALoS links for vehicles are provided in an obstructed environment. However, designing the flight path for rendering valid ALoS service is an NP-hard problem that is not feasible in real-time for autonomous navigation. We model the RISeUAV navigation as an optimization problem and propose an efficient technique to make the problem computationally tractable in real-time using Benders' decomposition method and sequential convex programming. Simulation results validate the effectiveness of the proposed method.**

***Index Terms*—Autonomous navigation, aerial LoS service, reconfigurable intelligent surfaces (RISs), optical communication, optimal trajectory, unmanned aerial vehicles (UAVs), wireless communication.**

I. Introduction

Modern generations of wireless communication networks (MWCNs) are being deployed to meet the bandwidth requirement of the drastic rise in data rate. The fifth-generation MWCNs, working under the quasi-optic millimeter-wave (mmWave) 3 – 300 GHz frequencies, have been exploited in some countries. Beyond that, the next generation of MWCN, working under 0.3 – 30000 THz falls within the optical spectrum constituting (visible light) optical wireless communication (OWC) [1]. OWC benefits from low-cost deployment, energy-efficient operation, and higher spectral efficacy with no health issues.

Although obviating the bandwidth concern, the performance of the 5G and OWC are limited to LoS links due to high propagation (path) loss and scattering. The multi-input multi-output (MIMO) active transmitters address the problem by establishing beamforming of the signals to the receivers but make the MWCNs complex and less efficient. The reconfigurable intelligent surface (RIS), acting as a passive component, is suggested to address the issue by phase shift/beamforming the incident signals in desired directions toward user equipment [2].

Equipping unmanned aerial vehicles (UAVs) with the RIS is a promising solution to provide aerial LoS (ALoS) service for critical security/police/rescue/emergency metropolitan services in dense urban areas covered by the 5G/optical MWCNs [3]. RIS-equipped UAVs (RISeUAVs) perform as aerial transponders that reflect the communication signals from base stations (BSs) to vehicles or for vehicle-to-vehicle communications. The excellent mobility of the UAVs helps to improve the robustness and convergence of the MWCNs for critical services. Besides, the RIS comprises passive elements to avoid complexity and onboard energy consumption that helps to reduce the cost/size/weight of the RISeUAV while improving its agility [4].

UAV navigation, path planning, and trajectory design have been broadly studied in the literature from the perspective of various applications [5]-[6]. However, the trajectory design of RISeUAV for the provision of the ALoS service for mobile vehicles is distinguished from the relevant literature as per the explanation given in the sequel.

- In most UAV-assisted communications, the UAV trajectory is designed in 2D space (at a fixed altitude) and for stationary receivers [7]. The objectives are exploring energy-efficient paths and power minimization for communication. In a limited of works, a mobile vehicle [3] and internet-of-vehicles have been considered [8]. However, obstacle-free paths and the ALoS service have not been considered.
- In robotic literature, obstacle-free path planning is studied in 2D and 3D environments. Various techniques for robotic path design have been examined such as Neural RRT* [9], nonlinear programming [10], Voronoi graph [11], etc. However, these methods are mostly for path planning and thus are not suitable for real-time applications. Besides, communication systems and LoS have not been considered.
- Obstacle-free 3D trajectory design through an obstructed dense urban area where the RISeUAV may fly among the buildings to provide ALoS service for moving vehicles has not been studied. Particularly, trajectory design for the navigation model should be programmed and solved in real-time to automate the navigation. However, the ALoS modeling and energy-efficient trajectory design is an NP-hard nonconvex problem considering uneven terrines.

To the best of the authors' knowledge, no work has elaborated on ALoS modeling and energy-efficient crash avoidance trajectory design for UAVs to provide ALoS service for moving nodes. Although spots, where ALoS is not available, can be regarded as obstacles/occupied state space that

This work was supported by the Australian Research Council. Also, this work received funding from the Australian Government, via grant AUSMURIB000001 associated with ONR MURI grant N00014-19-1-2571.

M. Eskandari and A. V. Savkin are with The School of Electrical Engineering and Telecommunications, University of New South Wales, Sydney, NSW 2052, Australia.

(*Corresponding author: Mohsen Eskandari*; m.eskandari@unsw.edu.au).

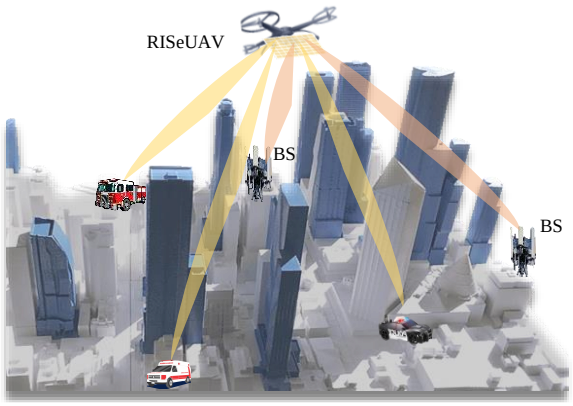

Fig. 1. The RIS-equipped UAVs (RISeUAVs) (RU) provides LoS communication service for mobile vehicles in 5G/optical MWCN.

should be avoided, ALoS modeling in the context of an optimization problem is an open research question. For instance, the necessity of ALoS modeling has been studied in [12] followed by geometrically modeling the ALoS region in Cartesian coordinates. Alternatively, authors in [13] consider the ALoS as a probabilistic equation for a UAV acting as an active base station. However, ALoS modeling has not been elaborated in the context of obstacle-free path planning which is an NP-hard optimization problem. In communication-relevant works, LoS has been identified by signal processing through deep learning methods and thus is not efficient for path planning and trajectory design [14].

This letter is the first work that 1) proposes and automates RISeUAV navigation through a dense urban area for providing ALoS service for mobile vehicles in obstructed 5G/optical MWCNs. For this purpose, the energy-efficient obstacle-free 3D trajectory design is modeled as an optimization problem. 2) After clarifying the computation hardness of the optimization problem for real-time programming, which is needed for autonomous navigation, the paper proposes an effective solution inspired by Benders' decomposition to address the time complexity, and successive convex programming approach is utilized to handle nonconvexity of the optimization problem.

The remainder of this paper is organized as follows. In Section II, the problem modeling and statement are presented. The proposed method for RISeUAV navigation is presented In Section III. Simulations are conducted in Section IV, and Section V concludes the paper.

II. Problem Statement

We consider one RISeUAV that renders ALoS service for multiple moving vehicles. Nevertheless, the scenario of multiple RISeUAVs supporting multiple vehicles (with ALoS service) can be decomposed to our case study where every RISeUAV covers a given region and the collaboration of the RISeUAVs can be coordinated by different methods [15].

The problem is planning an energy-efficient obstacle-free[1] trajectory for the RISeUAV while the ALoS service is maximized for the moving vehicles, see Fig. 1. Further velocity/acceleration and nonholonomic constraints must be satisfied. The trajectory planning is implemented in real-time at the UAV's overhead controller to make the navigation autonomous. To this end, the occupancy map of the covered urban area, including the coordinates of the BSs, is uploaded to the UAV's controller.

The RIS acts as an aerial reflector, so, there is no concern about optimizing power transmitted by the UAV. However, the phase shift of the RIS reflective elements must be optimally allocated to the vehicles. Also, the reliability of the ALoS service and data rate (i.e., the throughput of the communication via the ALoS link) are other concerns. In this light, there is a trade-off between flying at higher altitudes to increase the chance of providing ALoS links for more vehicles with keeping a low altitude for providing stronger ALoS channels for vehicles with higher data rates.

A. State Space Modeling

We model the state space in Cartesian coordinates. Let us model the position of the v^{th} vehicle at time τ is given by

$$p_v^{\mathcal{V}}(\tau) \coloneqq [x_v^{\mathcal{V}}(\tau),\ y_v^{\mathcal{V}}(\tau),\ z_v^{\mathcal{V}}(\tau)]^T \in \mathbb{R}^3, \tag{1}$$

where $x, y,$ and z denote Cartesian coordinates; $v \in \mathcal{V} = \{1, \dots, V\}$, and V denotes the number of vehicles, and superscript T is the matrix transpose operator. We assume that the vehicles are moving, and their map routes are frequently sent to the onboard (overhead) controller at the RISeUAV. The position of the b^{th} BS is given by

$$p_b^{\mathcal{B}} \coloneqq \left[x_b^{\mathcal{B}},\ \ y_b^{\mathcal{B}},\ \ z_b^{\mathcal{B}}\right]^T \in \mathbb{R}^3, \tag{2}$$

where $b \in \mathcal{B} = \{1, \dots, B\}$, B is the number of BSs in the area. For the RISeUAV (henceforth RU), let us define

$$p_m^{RU}(\tau) \coloneqq [x_m^{RU}(\tau),\ y_m^{RU}(\tau),\ z_m^{RU}(\tau)]^T \in \mathbb{R}^3, \tag{3}$$

where $m \in \mathcal{M} = \{1, \dots, M\}$ and M is the number of RIS elements. The RIS is facing the ground, see Fig. 2. Without loss of generality, we assume $p_m^{RU}(\tau) \coloneqq p^{RU}(\tau), \forall\, m \in \mathcal{M}$, where $p^{RU}(\tau)$ denotes the coordinates of the RISeUAV at time τ. Let $\vec{\Delta}_b^{BRU}(\tau) = p^{RU}(\tau) - p_b^{\mathcal{B}}(\tau)$ be the vector from the b^{th} BS to the RU and $\left|\vec{\Delta}_b^{BRU}(\tau)\right| = \left\|\vec{\Delta}_b^{BRU}\right\|$ denotes the vector length (i.e., the Euclidean distance); and the operator $\|\cdot\|$ is Euclidean norm. Similarly, we have $\vec{\Delta}_v^{RUV}(\tau) = p_v^{\mathcal{V}}(\tau) - p^{RU}(\tau)$ for the ALoS link between RU to vehicle v.

The RU movement is modeled via the following kinematic equation of motion:

$$\begin{bmatrix} \dot{p}^{RU}(t) \\ \dot{\theta}\ \ (t) \end{bmatrix} = \begin{bmatrix} \mathfrak{U}(t) \\ \omega(t) \end{bmatrix} + \begin{bmatrix} \mathbb{B} \\ 0 \end{bmatrix} u_0; \tag{4}$$

$$\mathfrak{U}(t) = [v_x(t),\ \ v_y(t),\ \ u(t)]^T;\ \ \mathbb{B} = [0 \quad 0 \quad -1]^T,$$

where $\theta(t)$ is the heading of the RISeUAV with respect to the $x-$axis; $v_x(t) = v(t)\cos\theta(t),\ v_y(t) = v(t)\sin\theta(t)$; $v(t)$, $u(t)$ and $\omega(t)$ denote linear horizontal, vertical, and angular speeds, respectively, $\mathfrak{U}(t)$ is the input (speed) to the RU navigation system and u_0 denotes minimum vertical input for hovering. Let $p_\Omega^{3D} \in \mathbb{R}^3$ be a set of coordinates of the occupancy map of the given urban area. The following condition validates the state space for the trajectory design

$$p^{RU}(\tau) \cap\ p_\Omega^{3D} = \emptyset\,. \tag{5}$$

Also, ALoS service should be available at the waypoints of the trajectory. For this, the ALoS link, at time instant τ, is modeled as

$$ALoS_{bv}(\tau) = \begin{cases} 1, & \left(\vec{\Delta}_b^{BRU}(\tau) \cup\ \vec{\Delta}_v^{RUV}(\tau)\right) \cap\ p_\Omega^{3D} = \emptyset \\ 0, & \left(\vec{\Delta}_b^{BRU}(\tau) \cup\ \vec{\Delta}_v^{RUV}(\tau)\right) \cap\ p_\Omega^{3D} \neq \emptyset \end{cases} \tag{6}$$

[1] By obstacle-free, we mean path planning while obviating collisions with buildings. Real-time path planning for autonomous navigation while considering dynamic obstacles (e.g., other UAVs) is an open research topic and is beyond the scope of this work.

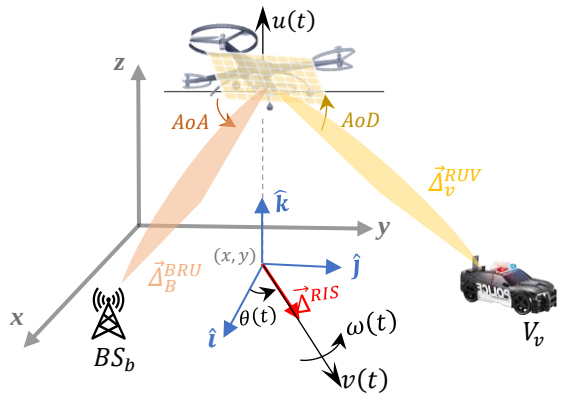

Fig. 2. The RISeUAV position and motion in the Cartesian coordinates.

$ALoS_{bv} = 1$ means the ALoS link is valid between the v^{th} vehicle and the b^{th} BS through RU, where $\vec{\Delta}_b^{BRU}$ and $\vec{\Delta}_v^{RUIV}$ denote the vector from the b^{th} BS to the RU, and the vector from the RU to the v^{th} vehicle, respectively. The $ALoS_{bv}(\tau)$ is validated by (linearly) interpolating the vectors and validating the intermediate points with the occupancy map. To this end, the normalized vector of a given vector, e.g., vector $\vec{\Delta}_b^{BRU}$, is obtained as

$$\partial_b^{BRU}\left((\zeta_b^{BRU}),(\varphi_b^{BRU})\right) = \begin{bmatrix}\cos(\zeta_b^{BRU})\cos(\varphi_b^{BRU})\\ \cos(\zeta_b^{BRU})\sin(\varphi_b^{BRU})\\ \sin(\zeta_b^{BRU})\end{bmatrix}^T; \quad (7)$$

where

$$\varphi_b^{BRU} = \cos^{-1}\left(\frac{x^{RU}-x_b^{\mathcal{B}}}{\left\|\left[(x^{RU}-x_b^{\mathcal{B}}),(y^{RU}-y_b^{\mathcal{B}})\right]^T\right\|_2}\right);$$

$$\zeta_b^{BRU} = \tan^{-1}\left(\frac{z^{RU}-z_b^{\mathcal{B}}}{\left\|\left[(x^{RU}-x_b^{\mathcal{B}}),(y^{RU}-y_b^{\mathcal{B}})\right]^T\right\|_2}\right).$$

Then, the i^{th} intermediate point is obtained as

$$p_b^{BRU}[k] = p_b^{B} + \partial_b^{BRU}\left((\zeta_b^{BRU}),(\varphi_b^{BRU})\right) \times \left(\frac{i}{\mathbb{I}}\left\|\vec{\Delta}_b^{BRU}\right\|\right); \quad (8)$$

where $\mathbb{I}$ is the number of intermediate segments. The larger $\mathbb{I}$ the more accurate results in the cost of computations burden.

B. ALoS Channel Performance

The free-space path loss channel model is used for the mmWave WCN in (5G)[2]. The channels gain matrix is given by

$$\Gamma_{BV}^{BRUV}(\tau) = \begin{bmatrix}\mathfrak{G}_{11}^{BRUV}(\tau) & \cdots & \mathfrak{G}_{1V}^{BRUV}(\tau)\\ \vdots & \ddots & \vdots\\ \mathfrak{G}_{B1}^{BRUV}(\tau) & \cdots & \mathfrak{G}_{BV}^{BRUV}(\tau)\end{bmatrix} \in \mathbb{R}^{B\times V} \quad (9)$$

where $\mathfrak{G}_{bv}^{BRUV}(\tau) = g_v^{RUV^{\mathcal{H}}}(\tau) \times \Theta(\tau) \times g_b^{BRU}(\tau)$;

$$g_b^{BRU}(\tau) = \frac{\sqrt{\rho}}{\left|\vec{\Delta}_b^{BRU}(\tau)\right|}\left[e^{-j\phi_{b(m=1)}^{BRU}(\tau)},\dots,e^{-j\phi_{bm}^{BRU}(\tau)},\dots,e^{-j\phi_{bM}^{BRU}(\tau)}\right]^T;$$

$$g_v^{RUV}(\tau) = \frac{\sqrt{\rho}}{\left|\vec{\Delta}_v^{RUV}(\tau)\right|}\left[e^{-j\phi_{(m=1)v}^{RUV}(\tau)},\dots,e^{-j\phi_{mv}^{RUV}(\tau)},\dots,e^{-j\phi_{Mv}^{RUV}(\tau)}\right]^T;$$

$\mathfrak{G}_{bv}^{BRUV}$ denotes the ALoS channel gain of the BS−RU−V link corresponding to the b^{th} BS and v^{th} vehicle; $g_b^{BRU}(\tau)$ and $g_v^{RUV}(\tau)$ denote channel gains of the BS−RU and RU−V links, respectively; $\phi_b^{BRU}(\tau) = \frac{2\pi}{\lambda}\left|\vec{\Delta}_b^{BRU}(\tau)\right|$ models the phase delay corresponding to the BS−RU channel and $\phi_v^{RUV}(\tau) = \frac{2\pi}{\lambda}\left|\vec{\Delta}_v^{RUV}(\tau)\right|$ models the phase delay corresponding to the RU−V channel; $\Theta(\tau)$ denotes the phase shift matrix of the RIS, and $\vartheta_m(\tau)$ denotes the phase shift of the m^{th} elements of the RIS, and $\mathcal{H}$ denotes Hermitian transpose. The equivalent ALoS channel gain $\mathfrak{G}_{bv}^{BRUV}$ (for the b^{th} BS and the v^{th} the vehicle) is obtained as:

$$\mathfrak{G}_{bv}^{BRUV} = \sum_{m\in\mathfrak{M}_v} ALoS_{bv}(\tau)\rho\frac{e^{j\left(\vartheta_m(\tau)+\left(\phi_v^{RUV}(\tau)-\phi_b^{BRU}(\tau)\right)\right)}}{\left|\vec{\Delta}_v^{RUV}(\tau)\right|\left|\vec{\Delta}_b^{BRU}(\tau)\right|}; \quad (10)$$

where $\mathfrak{M}_v$ is the number of RIS elements that are allocated to the v^{th} vehicle and should be optimally determined. The phase shift of the RIS reflectarrays can be adjusted to compensate for the delays in communicating signals through the ALoS link. Therefore, we may adjust the phase shift of the m^{th} element of the RIS as

$$\vartheta_m(\tau) = \left(\phi_b^{BRU}(\tau) - \phi_v^{RUV}(\tau)\right), \forall m \in \mathfrak{M}_v; \quad (11)$$

Consequently, after realizing the phase shift in (11) for a given number of RIS elements (i.e., $\mathfrak{M}_v$ associated with the vehicle v) the energies of the reflected signals are accumulated inherently at the vehicle v. Therefore, by plugging (11) into (10) the channel gain for the v^{th} vehicle connected to the b^{th} BS via RIS is obtained as

$$\mathfrak{G}_{bv}^{BRUV} = \frac{\rho\mathfrak{M}_v}{\left|\vec{\Delta}_v^{RUV}(\tau)\right| \times \left|\vec{\Delta}_b^{BRU}(\tau)\right|} = \frac{\rho\mathfrak{M}_v}{\|p_v^{\mathcal{V}}(\tau) - p^{RU}(\tau)\| \times \|p^{RU}(\tau) - p_b^{\mathcal{B}}(\tau)\|} \quad (12)$$

which reveals that the channel performance is impacted by the phase shift matrix and adversely affected by the ALoS length. Nevertheless, optimally determining $\mathfrak{M}_h$ is left as a problem objective which is studied in the next section. The achievable rate at vehicle v is calculated as

$$R_{bv}^{V}(\tau) = \log\left(1 + \left(\frac{P_b\left|\mathfrak{G}_{bv}^{BV}(\tau)+\mathfrak{G}_{bv}^{BRUV}(\tau)\right|^2}{\sigma^2}\right)\right); \quad (13)$$

where P_b denotes power transmitted by BS b; σ^2 is the noise power; $\mathfrak{G}_{bv}^{BV}(\tau) = \left(\sqrt{\rho}\tilde{g}/\left|\vec{\Delta}_{bv}^{BV}(\tau)\right|\right)$ denotes the channel gain of the direct BS−V link, and $\tilde{g}$ denotes random scattering.

C. Optimization Problem for RISeUAV Navigation

The problem objectives are 1) UAV energy minimization for mission endurance; 2) required reliability for establishing ALoS links for individual vehicles, and 3) data rate that needs stronger ALoS links with improved channel performance. The potential flight path is discretized into K segments with K time steps δ, for the time interval of interest $[t_0,\ t_0+\mathcal{T}]$. The three objectives are modeled as

$$\mathcal{J}_{eng} = \sum_{k=1}^{K}\mathcal{A}|\mathfrak{U}[k]|; \quad (14)$$

$$\mathcal{J}_{ALoS} = \sum_{k=1}^{K}\sum_{v=1}^{V}\sum_{b=1}^{B}(ALoS_{bv}[k]\times\alpha_{bv}[k]) \quad (15)$$

$$\mathcal{J}_{rate} = \sum_{k=1}^{K}\sum_{v=1}^{V}\sum_{b=1}^{B}\left(ALoS_{bv}[k]\times\alpha_{bv}[k]\times\mathfrak{G}_{bv}^{BRUV}[k]\right) \quad (16)$$

where $\mathcal{J}_{eng}$ denotes the energy consumption index for the

[2] In this paper, the ALoS channel model is developed in the context of mmWave communication in 5G, which is converted to the sequential convex optimization problem for trajectory planning and phase shift control, thanks to the RIS technology. Similarly, the optical RIS technology can be utilized to simplify the optimization model to trajectory design for providing ALoS links for more vehicles while minimizing UAV energy consumption. Therefore, optical channel model [1] is not elaborated in this work.

RISeUAV's propulsion and hovering; $\mathcal{A} = [\alpha_x,\ \alpha_y,\ \alpha_z]$ denote scaler coefficients to estimate consumed energy for UAV maneuvers from input speeds; $\mathcal{J}_{ALoS}$ counts the number of effective ALoS links, and $\mathcal{J}_{rate}$ models the channel performance through beamforming via RIS elements and minimizing the length of the ALoS links; $\alpha_{bv} \in \{0,1\}$ is an auxiliary binary variable which is 1 if vehicle v is connected to BS b through an ALoS link, and 0 otherwise; by which we aim to assign each vehicle to only one BS at each segment to avoid complexities associated with channel assignment and power control and resultant phase-shift algorithm. Since the RISeUAV provides additive communication links based on which the UAV navigation is designed, we consider maximizing the indirect ALoS channel gain in defining $\mathcal{J}_{rate}$ in (16), which maximizes the achievable rate due to the concavity of the logarithmic function in (13). Besides, for realizing a uniform achievable rate among vehicles we optimally distribute the phase shift matrix among vehicles (by determining $\mathfrak{M}_v$). To achieve the problem objectives, the optimization problem ($\mathcal{P}1$) is developed as

$$\mathcal{P}1: \quad \min_{\mathfrak{U}[k]} \gamma_{eng}\mathcal{J}_{eng},\ \max_{\mathfrak{U}[k],\mathfrak{M}_v[k],\alpha_{bv}[k]} \left(\gamma_{ALoS}\mathcal{J}_{ALoS} + \gamma_{rate}\mathcal{J}_{rate}\right)$$

$$s.t. \quad p^{RU}[k] = \left(p^{RU}[k-1] + \delta\,(\mathfrak{U}[k] + \mathbb{B})\right) \cap\ p_{\Omega}^{3D} = \emptyset; \quad (17)$$

$$Z_{min}^{RU} \le z[k] \le Z_{max}^{RU}; \quad (18)$$

$$0 \le v[k] = \left\| \left[v_x[k], v_y[k]\right]^T \right\|_2 < V_{max}^{RU},; \quad (19)$$

$$|u[k]| + \alpha_u |v[k]| < U_{max}^{RU}; \quad (20)$$

$$|\mathfrak{U}[k] - \mathfrak{U}[k-1]| < \delta\ \dot{\mathfrak{U}}_{max}^{RU}; \quad (21)$$

$$\left|\tan^{-1}\left(\frac{v_y[k]}{v_x[k]}\right) - \tan^{-1}\left(\frac{v_y[k-1]}{v_x[k-1]}\right)\right| < \frac{\delta \times W_{max}^{RU}}{1 + \alpha_\theta |v[k]|}; \quad (22)$$

$$\sum_{v=1}^{V} \mathfrak{M}_v[k] = M; \quad (23)$$

$$\frac{ALoS_{bv}[k]\alpha_{bv}[k]\mathfrak{M}_v[k]}{ALoS_{b'v'}[k]\alpha_{b'v'}[k]\mathfrak{M}_{v'}[k]} = \frac{\left|\vec{\Delta}_{v'}^{RUV}(\tau)\right|\left|\vec{\Delta}_{b'}^{\mathcal{B}RU}(\tau)\right|}{\left|\vec{\Delta}_{v}^{RUV}(\tau)\right|\left|\vec{\Delta}_{b}^{\mathcal{B}RU}(\tau)\right|} \quad (24)$$

$$\forall v, v' \in \mathcal{V};\ and\ \forall\ b, b' \in \mathcal{B};$$

$$0 \le \textstyle\sum_{b=1}^{\mathcal{B}} \alpha_{bv}[k] \le 1, \forall\ v \in \mathcal{V} \quad (25)$$

where γ_{eng}, γ_{ALoS}, and γ_{rate} are positive numbers to balance the problem objectives; Z_{min}^{RU} and Z_{max}^{RU} denote minimum and maximum permissible flight altitudes, respectively; V_{max}^{RU}, U_{max}^{RU}, and U_{max}^{RU} are maximum horizontal, vertical, and angular speeds, respectively; $\dot{\mathfrak{U}}_{max}^{RU} = \left[\dot{V}_{max}^{RU}(t),\ \dot{U}_{max}^{RU}(t),\ \dot{W}_{max}^{RU}(t)\right]^T$ denote maximum accelerations. Constraint (16) validates the state space for RISeUAV path planning; constraint (18) limits flight altitude; constraint (19) bounds horizontal speed; constraint (20) imposes a limit on the vertical speed, where α_u is a positive coefficient that adjusts UAV's vertical speed based on the horizontal speed and can be obtained from the UAV speed profile; constraint (21) bounds accelerations; constraint (22) imposes nonholonomic constraints (heading rate limit) based on the maximum angular speed and horizontal velocity of RISeUAV based on the positive coefficient α_θ given by the UAV flight data sheet; constraint (23) makes the sum of the allocated reflectarrays equal to the number of RIS elements; constraint (24) ensures reflectarrays are uniformly allocated among the vehicles that are provided with a valid ALoS link. To this end, as per the (12), $\mathfrak{M}_v$ is inversely proportional to the length of the corresponding ALoS link. The latter also bounds the solution to the phase shift optimization problem. Finally, constraint (25) makes sure that every vehicle is connected to only one BS (the corresponding BS that covers the vehicle's route).

D. NP-Hardness and Time Complexity of the Navigation Optimization Problem

The computation hardness of $\mathcal{P}1$ is discussed as follows:

1) The optimization problem $\mathcal{P}1$ is mixed integer in $\mathcal{J}_{ALoS}$ and (25) and nonconvex in $\mathcal{J}_{rate}$, (20), (22), and (24).
2) Modeling the valid ALoS link ($ALoS_{bv}$) as well as modeling the valid state space in (17) is not feasible in polynomial time to make the solution computationally tractable.
3) $\mathcal{P}1$ is a receding horizon predictive optimization problem and its performance depends on the number of finite receding horizons. To reach the optimal trajectory, the solutions to all segments must be optimized simultaneously, which is NP-hard, and the time complexity of the optimal solution is beyond the real-time programming.

III. The Proposed Navigation Model

To tackle the time complexity of the problem, we use Benders' decomposition method. First, we relax terms in the objective function and constraints that include complicating variables, i.e., ALoS link and valid state space. Therefore, we consider the optimization problem $\mathcal{P}2$ as

$\mathcal{P}2$:

$$\min_{\mathfrak{U}[k]} \left(\gamma_{eng}\mathcal{A}|\mathfrak{U}[k]| + \gamma'_{rate} \sum_{v=1}^{V} w_v[k] \left(\left\| p_v^{\mathcal{V}}[k] - p^{RU}[k] \right\|^2 \times \left\| p^{RU}[k] - p_{bv}^{\mathcal{B}}[k] \right\|^2 \right) \right);\ \forall k$$

$$s.t. \quad p^{RU}[k] = \left(p^{RU}[k-1] + \delta\,(\mathfrak{U}[k] + \mathbb{B})\right); \quad (26)$$

$$(18) - (22),$$

where $p_{bv}^{\mathcal{B}}[k]$ denotes the position of the BS associated with vehicle v at time instant k; γ'_{rate} is the updated value of the weighting coefficient due to the change in the objective function presenting the ALoS performance, and $w_v[k]$ is a positive coefficient to prioritize the provision of ALoS service for vehicle v. The solution to $\mathcal{P}2$ provides the optimum point in terms of minimizing energy consumption and the average lengths of individual BS−RU−V ALoS links. For the obtained point, the obstacle-free and valid state-space constraints are checked using (5). If these state-space constraints are not satisfied, then we put cuts on the XY-plane of the local state-space area until it is validated by the nonholonomic (heading rate) constraint in (22). Then we check for the ALoS links using (6)-(8), if the ALoS links are not valid for all/some of the vehicles, we put a cut to Z-axes, i.e., increase the flight altitude to provide ALoS links for all vehicles. If we reach a maximum altitude while ALoS still has not been valid for some vehicles, we update $w_v[k+1]$ to prioritize the vehicles for the receding time steps.

Remark 1. Since the spatio-temporal variability of vehicles is bounded, the solution to $\mathcal{P}2$ provides the optimal trajectory (considering the energy consumption and ALoS communication channel performance with motion and nonholonomic constraints) while Benders' cuts validate ALoS links and obstacle-free path. Therefore, we do not consider the predictive receding horizon in $\mathcal{P}2$ since the Benders' cuts converge the solution to the optimal valid trajectory.

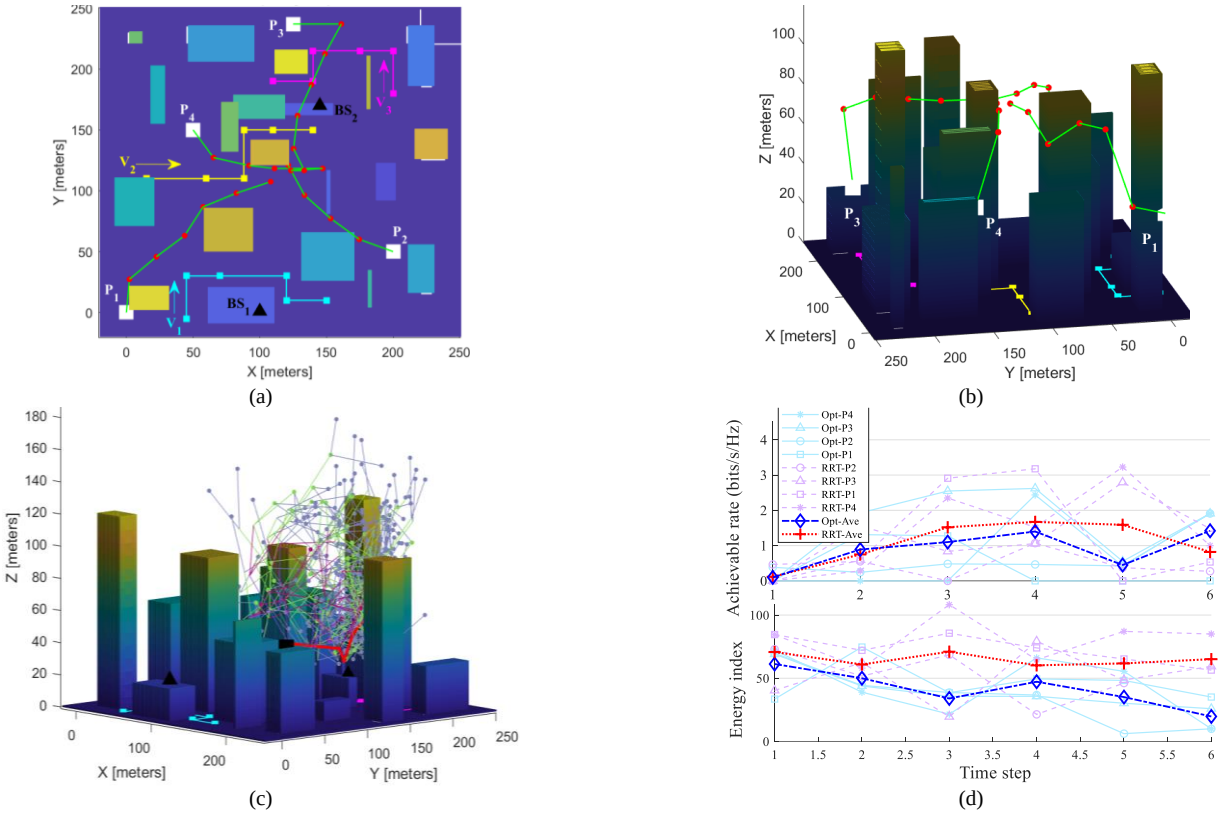

Fig. 3. Simulation results: (a) Map routes of three vehicles in the XY plane (waypoints are indicated by squares); red dots connected by green lines indicate the designed trajectory of RISeUAV for different start positions; (b) optimal trajectories in 3D schematic; (c) explored trajectory (with red color) for start position p_2 given by the sampling-based RRT method; (d) performance comparison of the proposed optimization (Opt.) method and RRT for energy consumption index and the average achievable rates at vehicles. The average results (Opt-Ave and RRT-Ave) are presented for clear comparison.

After obtaining the optimal position for the given time slot, the RIS elements are optimally allocated to the vehicles by solving $\mathcal{P}3$ as follows

$$\mathcal{P}3: \quad \max_{\mathfrak{M}_v} \sum_{v=1}^{V} \frac{\mathfrak{M}_v}{\|p_v^{\mathcal{V}}[k]-p^{RU}[k]\|\times\|p^{RU}[k]-p_{bv}^{\mathcal{B}}[k]\|}$$
$$s.t. \quad (23)-(24)$$

where the denominator of $\mathcal{P}3$ is known after achieving the solution of $\mathcal{P}2$; therefore $\mathcal{P}3$ is solvable by linear programming.

A. *The Solution to $\mathcal{P}2$ with Benders' Cuts*

Optimization problem $\mathcal{P}2$ is non-convex due to the product of two Euclidean norms in the objective function and constraint (22). To make it tractable we develop $\mathcal{P}2\_a$ problem as

$$\mathcal{P}2_a: \min_{\mathfrak{U}[k]} \left(\gamma_{eng}\mathcal{A}\left|\mathfrak{U}^{(i)}[k]\right| + \gamma'_{rate} \sum_{v=1}^{V} w_v[k] \times \left\|\delta\mathfrak{U}^{(i)}[k] - \Delta p_v^{RU}[k]\right\|^2 \right);$$

$$s.t. \quad \beta^{(i)}\left(p^{RU}[k-1] + \delta\left(\mathfrak{U}^{(i)}[k]+\mathbb{B}\right) - P_{Lim}^{(i)}[k]\right) < 0; \quad (27)$$

$$(|u[k] + \alpha_u v[k-1]u[k]|) < U_{max}^{RU}; \quad (28)$$

$$\begin{bmatrix} v_x[k] \\ v_y[k] \end{bmatrix} - \left(1 - \frac{1}{V_{max}^{RU}}\right)\begin{bmatrix} v_x[k-1] \\ v_y[k-1] \end{bmatrix} > 0; \quad (29)$$

$$(18)-(19) \text{ and } (21),$$

where $\Delta p_v^{RU}[k] = p_v^{\mathcal{V}}[k] - (p^{RU}[k-1] + \delta\mathbb{B})$; superscript (i) denotes Benders' iteration; $\beta^{(i)} = diag\left\{\beta_x^{(i)}, \beta_y^{(i)}, \beta_z^{(i)}\right\}$;

$$\beta_x^{(i)} = \begin{cases} +1, & x^{*(i-1)}[k] \in p_\Omega^{3D} \text{ and } x^{RU}[k-1] < x^{*(i-1)}[k] \\ 0, & x^{*(i-1)}[k] \notin p_\Omega^{3D} \text{ or } v_x^{*(i-1)}[k] > v_y^{*(i-1)}[k] \\ -1, & x^{*(i-1)}[k] \in p_\Omega^{3D} \text{ and } x^{RU}[k-1] > x^{*(i-1)}[k] \end{cases};$$

$$\beta_y^{(i)} = \begin{cases} +1, & y^{*(i-1)}[k] \in p_\Omega^{3D} \text{ and } y^{RU}[k-1] < y^{*(i-1)}[k] \\ 0, & y^{*(i-1)}[k] \notin p_\Omega^{3D} \text{ or } v_x^{*(i-1)}[k] \le v_y^{*(i-1)}[k] \\ -1, & y^{*(i-1)}[k] \in p_\Omega^{3D} \text{ and } y^{RU}[k-1] > y^{*(i-1)}[k] \end{cases};$$

$$\beta_z^{(i)} = \begin{cases} 1, & z^{*(i-1)}[k] \in p_\Omega^{3D} \text{ or } LoS_{bv}[k] < V \text{ and } u^{*(i)}[k] < U_{max} \\ 0, & z^{*(i-1)}[k] \notin p_\Omega^{3D} \text{ or } z^{*(i-1)}[k] > Z_{max}^{RU} \text{ or } u^{*(i)}[k] > U_{max} \end{cases};$$

$$P_{Lim}^{(i)}[k] = \begin{bmatrix} X_{Lim}^{(i)} \\ Y_{Lim}^{(i)} \\ Z_{Lim}^{(i)} \end{bmatrix} = \begin{cases} P_{Lim}^{(i-1)}[k] - \beta^{(i)}\kappa, & (i)=1 \\ p^{*(i-1)}[k] - \beta^{(i)}\kappa, & (i)>1 \end{cases};$$

$p^{*(i-1)}[k] = \left[x^{*(i-1)}[k], y^{*(i-1)}[k], z^{*(i-1)}[k]\right]^T = p^*[k-1] + \delta\left(\mathfrak{U}^{*(i-1)}[k] + \mathbb{B}\right)$ is the optimal trajectory waypoint at the time step k and iter $(i-1)$, and $\kappa \in \mathbb{R}$ is a positive number specified based on the resolution of the occupancy map.

Constraint (27) models Benders' cuts, constraints (28)-(29) limit vertical speed and heading rate based on horizontal speed. $\mathcal{P}2_a$ can be solved by linearizing the L2-norm term around the local point applying Taylor expansion or can be solved by convex programming (e.g., the interior-point method). Then we solve $\mathcal{P}2_b$ and the final solution would be the average of solutions to $\mathcal{P}2_a$ and $\mathcal{P}2_b$, where

$$\mathcal{P}2_b: \min_{\mathfrak{U}[k]} \left(\gamma_{eng}\mathcal{A}\left|\mathfrak{U}^{(i)}[k]\right| + \gamma'_{rate} \sum_{v=1}^{V} w_v[k] \times \left\|\delta\mathfrak{U}^{(i)}[k] - \Delta p_{bv}^{RU}[k]\right\|^2 \right)$$

$$s.t. \quad (18)-(19), (21) \text{ and } (27)-(29)$$

where $\Delta p_{bv}^{RU}[k] = p_{bv}^{\mathcal{B}}[k] - (p^{RU}[k-1] + \delta\mathbb{B})$.

B. Time Complexity of the Proposed Optimization Model

The time complexity of the trajectory design with the sampling-based (e.g., RRT) method is impacted by the problem objectives and constraints and can be approximated by

$$T_{RRT}(N) = T_{Sample} + T_{ALoS} + T_{Obstacle} + T_{OF} + T_{Constraints};$$

$$T_{RRT}(N) \approx \mathcal{O}\left(\sum_{k=1}^{K} N(k)\right) + \mathcal{O}\left(\sum_{k=1}^{K} N(k)V\mathbb{I}\right) + \mathcal{O}\left(\prod_{k=1}^{K-1} log(N(k)\,\mathbb{I})\right) + \mathcal{O}\left(\prod_{k=1}^{K-1} log\big(N(k)\big)\right) + \mathcal{O}\left(2\prod_{k=1}^{K-2} log\big(N(k)\big)\right).$$

where $N(k)$ denotes the number of random samplings in time step k, and V is the number of vehicles. Whereas the time complexity of the proposed method is

$$T(N) = \big(\mathcal{O}(K\,\mathcal{P}2_a) + \mathcal{O}(K\,\mathcal{P}2_b) + \mathcal{O}(K\,\mathcal{P}3)\big) \approx \mathcal{O}\left(2K\,V\,\mathbb{I}\log\left(\frac{1}{\varepsilon_0}\right)\right) + \mathcal{O}(K\,V);$$

where $\mathbb{I}$ denotes the resolution of the linear interpolation method, and ε_0 denotes iteration accuracy of the interior-point method. The proposed method reveals a more computationally efficient performance.

IV. Simulation Results

The proposed real-time navigation method is evaluated by computer-based simulation results in Matlab. The system parameters are $P_b = 20$ dBm, $\sigma^2 = -80$ dBm, $\rho = -30$ dB, $M = 900$. The speed constraints are $V_{max} = 12\frac{m}{s}, U_{max} = 8\frac{m}{s}, W_{max} = \pi/9\ \frac{rad}{slot}$. The 3D map of the urban area is shown in Fig. 3. Three vehicles (V_1, V_2, and V_3) move in arbitrary directions that are covered by two BSs (BS_1, BS_2). The vehicle routes are discretized into 6 waypoints including start/endpoints. Therefore, there are six time steps, 5 seconds each. Four different start positions are considered for the RISeUAV (P_1, P_2, P_3, and P_4). The performance of the proposed method for designing obstacle-free paths is illustrated in Fig. 3(a) which shows the XY-plane. Also, the convergence of all trajectories to the optimal points for the last time steps (while considering different initial positions and motion constraints) reveals the effectiveness of the navigation model to explore the optimal trajectory, see Fig. 3(b). The average computation time, recorded by the Matlab $tic\ toc$ function is less than 1 second (when neglecting ALoS links) and 11.34 seconds in total, which is acceptable for real-time autonomous navigation considering that the total flight time is 25 seconds. This implies the importance of efficient LoS modeling for optimization purposes, which is an NP-hard problem. The simulation results for the RRT* method [3] for the same conditions as the start position P_2 is shown in Fig. 3(c), which took 325.4 seconds to explore the optimal path. The performance comparison is illustrated in Fig. 3(d), where the proposed method reveals better performance in terms of the energy index and comparable results for the achievable rate, notice that the computational burden of the proposed method is far less than RRT. It makes the proposed method effective and efficient for real-time trajectory planning to automate the RISeUAV navigation.

V. Conclusion

The energy-efficient crash avoidance 3D navigation of the RISeUAV was studied for delivering ALoS service to mobile vehicles in obstructed dense urban areas covered by 5G/optical MWCNs. The navigation model was developed as an optimization problem by considering the energy consumption by UAV and the ALoS channel performance as the optimization objectives where crash-avoidance, valid ALoS links, and UAV speed/nonholonomic limits were constraints. The NP-harness and nonconvexity of the problem were clarified followed by proposing an effective method to make the problem solvable in real-time to automate the RISeUAV flight for ALoS service. The proposed method was validated through computer-based simulations. Future work can study and compare the performance of different interpolating methods to handle the computational hardness of the optimization problem that arose for modeling valid ALoS links.

References

[1] A. Al-Kinani, C. -X. Wang, L. Zhou and W. Zhang, "Optical Wireless Communication Channel Measurements and Models," in *IEEE Comm. Surveys & Tutorials*, vol. 20, no. 3, pp. 1939-1962, 2018.

[2] H. Zhang, B. Di, L. Song and Z. Han, "Reconfigurable Intelligent Surfaces Assisted Communications With Limited Phase Shifts: How Many Phase Shifts Are Enough?," in *IEEE Trans. on Veh. Tech.*, vol. 69, no. 4, pp. 4498-4502, April 2020.

[3] M. Eskandari, H. Huang, A. V. Savkin, and W. Ni, "Autonomous Guidance of an Aerial Drone for Maintaining an Effective Wireless Communication Link with a Moving Node using an Intelligent Reflecting Surface, " *2022 14th Int. Conf. on Computer and Aut. Eng. (ICCAE).*

[4] M. Samir, M. Elhattab, C. Assi, S. Sharafeddine and A. Ghrayeb, "Optimizing Age of Information Through Aerial Reconfigurable Intelligent Surfaces: A Deep Reinforcement Learning Approach," in *IEEE Trans. on Veh. Tech.*, vol. 70, no. 4, pp. 3978-3983, April 2021.

[5] X. Zhou, Q. Wu, S. Yan, F. Shu and J. Li, "UAV-Enabled Secure Communications: Joint Trajectory and Transmit Power Optimization," in *IEEE Trans. on Veh. Tech.*, vol. 68, no. 4, pp. 4069-4073, April 2019.

[6] X. Zhou, X. Yu, Y. Zhang, Y. Luo and X. Peng, "Trajectory Planning and Tracking Strategy Applied to an Unmanned Ground Vehicle in the Presence of Obstacles," in *IEEE Trans. on Aut. Sc. and Eng.*, vol. 18, no. 4, pp. 1575-1589, 2021.

[7] Y. Zeng, J. Xu and R. Zhang, "Energy Minimization for Wireless Communication With Rotary-Wing UAV," in *IEEE Trans. on Wireless Comm.*, vol. 18, no. 4, pp. 2329-2345, April 2019.

[8] X. Liu, B. Lai, B. Lin and V. C. M. Leung, "Joint Communication and Trajectory Optimization for Multi-UAV Enabled Mobile Internet of Vehicles," in *IEEE Trans. on Intellig. Transp. Syst.*, 2021.

[9] J. Wang, W. Chi, C. Li, C. Wang and M. Q. -H. Meng, "Neural RRT*: Learning-Based Optimal Path Planning," *IEEE Trans. on Aut. Sc. and Eng.*, vol. 17, no. 4, pp. 1748-1758, 2020.

[10] J. Li, M. Ran and L. Xie, "Efficient Trajectory Planning for Multiple Non-Holonomic Mobile Robots via Prioritized Trajectory Optimization," in *IEEE Rob. and Aut. Letters*, vol. 6, no. 2, pp. 405-412, April 2021.

[11] J. Wang and M. Q.-H. Meng, "Optimal Path Planning Using Generalized Voronoi Graph and Multiple Potential Functions," in *IEEE Trans. on Ind. Electron*, vol. 67, no. 12, pp. 10621-10630, 2020.

[12] J. Sabzehali, V. K. Shah, H. S. Dhillon and J. H. Reed, "3D Placement and Orientation of mmWave-Based UAVs for Guaranteed LoS Coverage," in *IEEE Wireless Com. Letters*, vol. 10, no. 8, pp. 1662-1666, Aug. 2021.

[13] A. Meng, X. Gao, Y. Zhao and Z. Yang, "Three-Dimensional Trajectory Optimization for Energy-Constrained UAV-Enabled IoT System in Probabilistic LoS Channel," in *IEEE IoT J.*, vol. 9, no. 2, 1109-1121, 2022.

[14] Q. Zheng *et al.*, "Channel Non-Line-of-Sight Identification Based on Convolutional Neural Networks," in *IEEE Wireless Com. Letters*, vol. 9, no. 9, pp. 1500-1504, Sept. 2020.

[15] M. Eskandari, A. V. Savkin and W. Ni, "Consensus-Based Autonomous Navigation of a Team of RIS-Equipped UAVs for LoS Wireless Communication With Mobile Nodes in High-Density Areas," in *IEEE Transactions on Automation Science and Engineering*, Early Access, 2022, doi: 10.1109/TASE.2022.3183335.